Article

TRANSPARENT PROCESS

EMBO reports

Bacilli glutamate dehydrogenases diverged via coevolution of transcription and enzyme regulation

Lianet Noda-Garcia[1], Maria Luisa Romero Romero[1], Liam M Longo[1], Ilana Kolodkin-Gal[2] & Dan S Tawfik[1,*]

Abstract

The linkage between regulatory elements of transcription, such as promoters, and their protein products is central to gene function. Promoter–protein coevolution is therefore expected, but rarely observed, and the manner by which these two regulatory levels are linked remains largely unknown. We study glutamate dehydrogenase—a hub of carbon and nitrogen metabolism. In *Bacillus subtilis*, two paralogues exist: GudB is constitutively transcribed whereas RocG is tightly regulated. In their active, oligomeric states, both enzymes show similar enzymatic rates. However, swaps of enzymes and promoters cause severe fitness losses, thus indicating promoter–enzyme coevolution. Characterization of the proteins shows that, compared to RocG, GudB's enzymatic activity is highly dependent on glutamate and pH. Promoter–enzyme swaps therefore result in excessive glutamate degradation when expressing a constitutive enzyme under a constitutive promoter, or insufficient activity when both the enzyme and its promoter are tightly regulated. Coevolution of transcriptional and enzymatic regulation therefore underlies paralogue-specific spatio-temporal control, especially under diverse growth conditions.

Keywords *Bacillus subtilis*; enzyme evolution; glutamate dehydrogenases; paralogue specialization

Subject Categories Evolution; Metabolism; Microbiology, Virology & Host Pathogen Interaction

DOI 10.15252/embr.201743990 | Received 25 January 2017 | Revised 23 March 2017 | Accepted 27 March 2017 | Published online 3 May 2017

EMBO Reports (2017) 18: 1139–1149

See also: **B van Loo & E Bornberg-Bauer** (July 2017)

Introduction

The regulation of gene activity is fundamental to life and a key to evolutionary innovation [1]. Gene duplication is the primary source of new genes as indicated by the dominance of paralogues, in eukaryotes but also in prokaryotes. Accordingly, recently diverged paralogues (≥ 75% sequence identity, as are the *B. subtilis* paralogues studied here) comprise a significant fraction of prokaryotic genomes (2.5–50%) [2]. Regulation of expression may account for the functional specialization of most duplicated genes [3], and accordingly, up to 40% of paralogues exhibit different expression profiles [4–6]. Nonetheless, new paralogues typically exhibit accelerated evolutionary rates in both their regulatory and coding regions [7–9]. The current literature separately addresses the action of natural selection on regulatory regions and on coding regions, with weak or no indications of coadaptation [4,10,11]. In some cases, paralogues with different expression profiles and different biochemical functions have been described [12–15]. However, the co-adaptation of these two traits has not been noted. Here, we describe a case study, showing that evolutionary changes occurred in both the enzymes and in their transcriptional regulation, and that the changes in these two traits are highly correlated.

Our case study addresses two *Bacillus subtilis* glutamate dehydrogenase (GDH) paralogues named RocG and GudB [16] (Fig 1A). We chose *Bacillus subtilis* because of its ecological diversity, and GDHs because they are central to nitrogen and carbon metabolism and are tightly regulated [17]. GDHs are only active as hexamers and are allosterically regulated by a range of metabolites, including amino acids and ATP [18] (Fig 1B). RocG and GudB are catabolic, NAD^+-utilizing GDHs that catalyse the reductive deamination of glutamate, thereby enabling direct utilization of glutamate as carbon and nitrogen source, or utilization of other amino acids such as arginine or proline via glutamate-coupled pathways [19] (Fig 1C). The coding sequences of RocG and GudB are ~75% identical. RocG is named after its genomic localization next to arginine catabolic genes. Studies of the domesticated strain *B. subtilis* 168 indicated that transcription of RocG is tightly coordinated: RocG is downregulated during glucose utilization (catabolic repression) and exponential growth [20,21] and upregulated when amino acids such as arginine are available as carbon and nitrogen sources [22–25] (gene: RocG; http://www.subtiwiki.uni-goettingen.de) (Appendix Fig S1). In contrast, GudB is expressed under a strong constitutive promoter with no indication of nitrogen-associated regulation or catabolic repression [16]. Accordingly, GudB's genomic location, although conserved, is not associated with other nitrogen metabolic genes. In the domesticated *B. subtilis* strain studied to date, GudB is cryptic due to an insertion that renders the enzyme inactive [16,26]. Thus,

1 Department of Biomolecular Sciences, Weizmann Institute of Science, Rehovot, Israel
2 Department of Molecular Genetics, Weizmann Institute of Science, Rehovot, Israel
*Corresponding author. Tel: +972 8 934 3637; E-mail: dan.tawfik@weizmann.ac.il

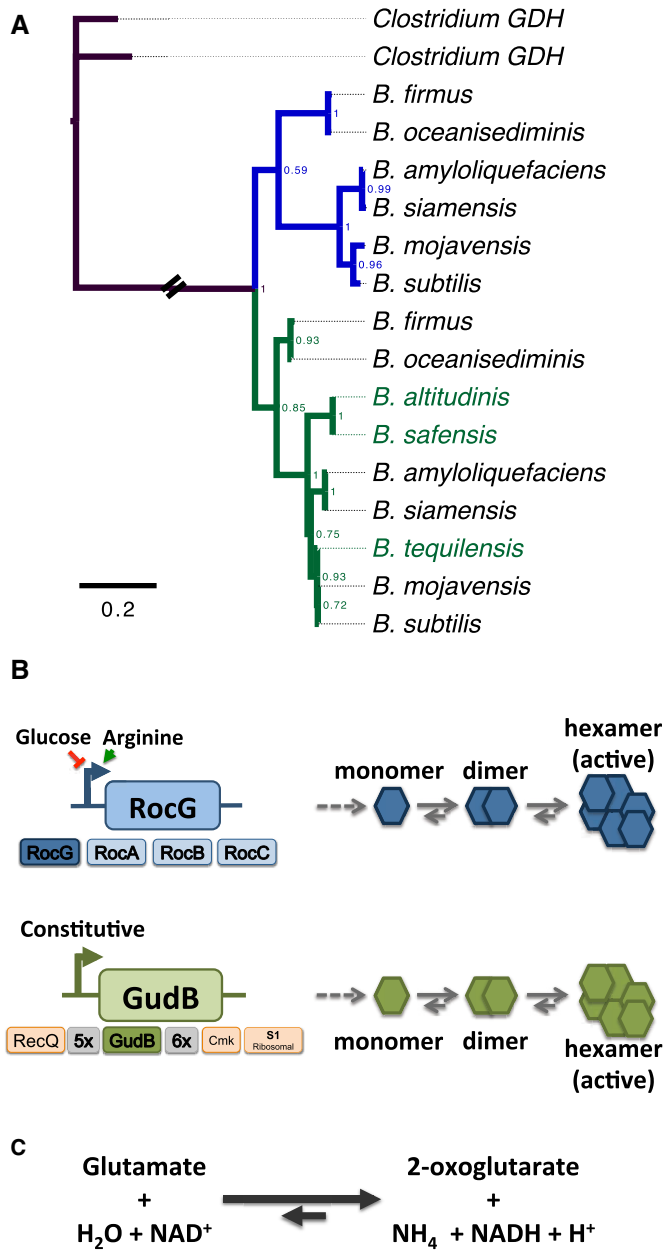

Figure 1. RocG and GudB: a schematic view of the two *Bacilli* glutamate dehydrogenase paralogues.

A A representative tree showing the RocG and GudB genes along the *Bacillus* genus (the NAD^+-specific GDH of *Clostridia* was used as out-group [51]; for a comprehensive analysis see Appendix Table S1). The scale bar shows amino acid substitutions per site. The blue branches correspond to RocG, and the green ones to GudB; this colour scheme is used throughout this paper. Species denoted in green lost the RocG paralogue. This study focussed on RocG and GudB from *Bacillus subtilis* NCIB 3610.

B, C A schematic representation of (B) the genomic context, transcriptional regulation, oligomeric structure and (C) enzymatic activity of RocG and GudB.

the interplay between these two paralogous GDHs remains unknown.

Studying wild-type *B. subtilis* NCIB 3610, in which both RocG and GudB encode active enzymes [26], we found that RocG and GudB knockouts exhibit different phenotypes, and that these phenotypes cannot be accounted for by differences in the promoters or the enzymes on their own. Combining genetic and biochemical studies, we explored the molecular basis of promoter–enzyme coevolution in the *Bacilli* GDHs. Our findings indicate that, in contrast to the tight transcriptional regulation of RocG, GudB's regulation occurs primarily at the enzyme level. Notably, GudB's enzymatic activity, and to a lesser extent RocG's, is regulated via assembly of hexamers from inactive subunits, rather than by the commonly described allosteric regulation. Assembly is prompted by the cooperative effect of high glutamate and basic pH.

Results

GudB and RocG's transcription profiles and protein levels

Previous characterization of RocG and GudB's transcription was performed in the domesticated strain in which GudB is non-functional. Wild-type *B. subtilis* strains, including strain NCIB 3610 studied here, encode a functional GudB [26,27]. By constructing strains in which RocG and GudB's coding regions were replaced with a GFP reporter, we found that RocG's transcription in the wild-type strain is tightly regulated, as observed in the domesticated strain [16]. Specifically, in both liquid and solid media, activation of the RocG promoter was only observed when arginine was used as carbon and nitrogen source (Fig 2A and Appendix Fig S2). GudB's transcription was not only much higher than RocGs (up to 30-fold), but also remained high in all conditions tested, including in glucose–ammonia as carbon–nitrogen source (Fig 2A and Appendix Fig S2), a medium where GDH activity is unnecessary (shown in the next section).

In agreement with the observed transcriptional levels, GudB's soluble monomers were detected by an immunoblot using polyclonal antibodies raised against recombinant GudB, under all conditions including in glucose–ammonia (Fig 2B). As expected, RocG was detected in cells grown in an arginine-containing medium, to a much lesser extent in a medium with proline, and not detected when cells were grown on glucose–ammonia. The levels of soluble RocG monomers seem to increase in the GudB knockout (Δ*gudB*, see below), suggesting a degree cross-regulation. However, the mutual cross-reactivity of GudB (Dr. Ulf Gerth, personal communication) and RocG antibodies [25], also observed here (Fig 2B), precludes precise quantification.

GudB and RocG phenotypes

To test how the different expression patterns affect growth, single and double knockouts of *B. subtilis rocG* and *gudB* genes were constructed in *B. subtilis* NCIB 3610. Their growth rates were compared to wild-type under various conditions. First, glucose–ammonia was used as carbon and nitrogen sources, where GDH catabolic activity is unnecessary [16]. Accordingly, all knockouts showed wild-type-like growth rates in liquid and also reached the wild type's colony size on solid media (Fig 3, top panel). Notably, and contrary to what had been observed with the domesticated *B. subtilis* [16,26], we observed no improved growth for the GudB knockout in glucose–ammonia as one might expect from the fact

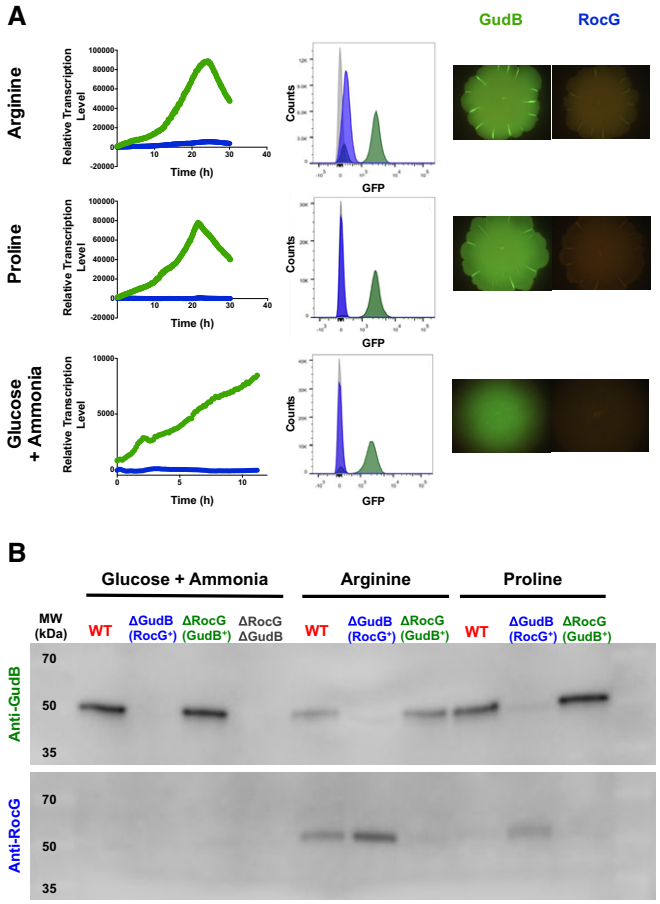

Figure 2. Expression profiles of GudB and RocG.

A GudB (in green) and RocG (blue) transcription levels were determined by replacing the enzymes' ORFs with a GFP reporter. Left: Growth in liquid MS media with different nitrogen–carbon sources. The growth rates of all strains were identical (Appendix Fig S8), and thus, transcription levels are presented as the ratio of GFP florescence ($OD_{535\ nm}$) to cell density ($OD_{600\ nm}$). Each point is the result of two biological replicates and ≥ 16 technical replicates; SD values are shown in Appendix Fig S8. Centre: GFP fluorescence levels in cells grown on solid media containing different nitrogen–carbon sources. Cell derived from the agar colonies shown on the right was suspended in buffer and analysed by flow cytometry (the wild-type strain is shown in grey). Shown are histograms for gated events (high fluorescence events; non-gated histograms are available in Appendix Fig S2).

B Western blot analysis of GudB and RocG levels in the different strains and under different growth conditions. Cells were harvested at the end of the logarithmic phase (OD_{600} ~ 0.8). Twenty micrograms of total soluble cell protein was applied per lane. GudB and RocG were detected with the corresponding polyclonal antibodies (anti-RocG [25] and anti-GudB (kindly provided by Dr. Ulf Gerth)).

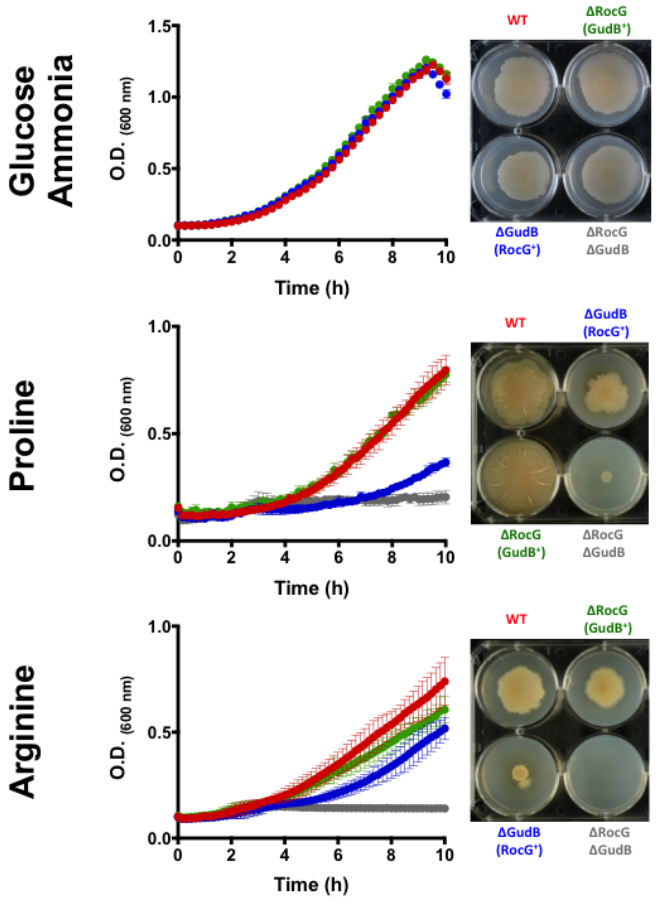

Figure 3. RocG and GudB phenotypes with different carbon–nitrogen sources.

Growth of the single (Δ*gudB*, Δ*rocG*) and the double (Δ*gudB* Δ*rocG*) knockout strains was monitored in liquid MS medium (left) or on agar plates (right), with different carbon–nitrogen sources. Red, wild-type; blue, Δ*gudB* ($RocG^+$); green, Δ*rocG* ($GudB^+$); grey, Δ*gudB*_Δ*rocG* (double knockout). Error bars represent the standard deviation (SD) observed in four independent experiments.

that under this condition, and as confirmed below, excessive GDH activity is deleterious.

When GDH activity is needed, GudB seems to be the major provider. With proline as nitrogen source, Δ*rocG* grows like wild type, while Δ*gudB* grows slower (Fig 3, mid panel). The double knockout, Δ*gudB*_Δ*rocG*, showed almost no growth. Thus, in proline, RocG's contribution is relatively minor, in agreement with RocG's transcription being triggered primarily by arginine. Indeed, when arginine was used as the carbon and nitrogen source, the knockout of RocG had a notable, deleterious effect on growth (Fig 3, bottom panel). Nonetheless, even in arginine, GudB seems to have a larger contribution to growth than RocG, as indicated by the larger deleterious knockout effects in both liquid and solid media. Thus, in the presence of either arginine or proline, GudB appears to be the major provider of GDH activity. Two additional lines of evidence support this conclusion: first, GudB expression levels are 10-fold (and up to 30-fold) higher than those of RocG (Fig 2A); second, RocG is preferentially lost in many *Bacillus* species that retain GudB, including species closely related to *B. subtilis* (Appendix Table S1 and Fig 1).

In agreement with the scenario that the relative contribution of RocG and GudB to glutamate catabolism correlates primarily with their transcriptional levels, we found that RocG and GudB have comparable K_M and k_{cat} values. Overall, their k_{cat}/K_M values differ by a factor of 3.7 in favour of RocG (owing to an approximately six times lower K_M, yet ~1.7 times lower k_{cat}; Fig 4). Thus, at glutamate concentrations above 5 mM, GudB's turnover rate is expected to be somewhat faster than RocG's.

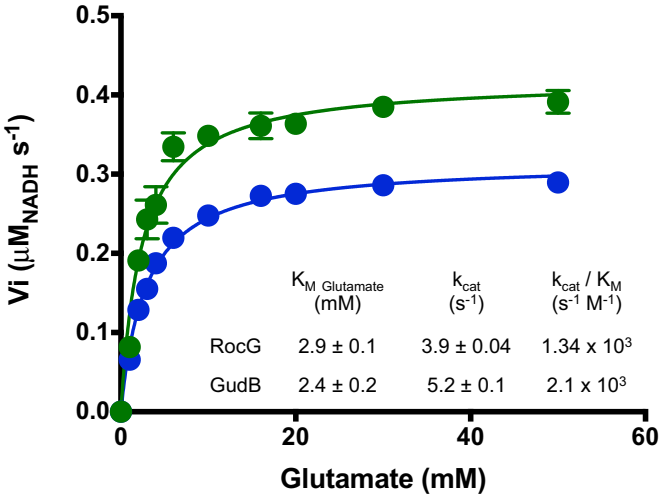

Figure 4. Kinetic parameters of RocG and GudB in their pre-assembled oligomeric states.

Initial rates of enzymatic conversion of glutamate to 2-oxoglutarate were measured by the rates of reduction of NAD^+ into NADH. Aliquots of stock solutions of the concentrated enzymes in their hexameric states were directly added to a reaction buffer with 4 mM NAD^+ and different concentrations of glutamate. Initial rates were determined by absorbance at 340 nm. The final enzyme concentration used was 0.05 μM (enzyme concentrations and k_{cat} values relate to subunit, i.e. monomer protein concentrations). Data were fit to Michaelis–Menten model. Error bars represent the SD observed in three independent experiments.

Promoter–enzyme incompatibility

Promoters are usually the key to transcriptional regulation in bacteria. However, it was shown that RocG's regulation is also affected by a so-called downstream activating sequence [22]. The similarity in catalytic efficiencies of GudB and RocG suggests that their regulatory, non-coding regions (promoter–terminator) diverged with little, if any, adaptive changes in their coding region. This scenario would be validated if swapping between non-coding regions and open-reading-frames (ORFs) shows no fitness effects; that is, the contribution of RocG and GudB to growth should remain the same upon exchanging their ORFs while retaining the original promoter–terminator regions (e.g. [3]). Thus, chimeric constructs of the ORFs and non-coding regions of the *rocG* and *gudB* genes were constructed as schematically presented in Fig 5A. Both, the 5′ and 3′ untranslated regions were included, as RocG's transcription is activated by the 3′ untranslated region [22]. The wild-type and swapped-gene constructs were inserted at a neutral landing site into the genomes of the Δ*gudB*_Δ*rocG* strain (thus isolating the effect of a single GDH gene) and also into the genomes of Δ*gudB* and Δ*rocG* (to generate a wild-type-like background with two paralogous GDHs). Growth curves of all constructs were obtained and these supported the conclusions described below (Appendix Fig S3). However, because the growth curves of *B. subtilis* in some media show more than a single exponential phase (Appendix Fig S3), and to enable accurate measurements of fitness differences, we performed competition experiments upon serial growth passages. Strains carrying the original or the swapped genes were expressed with a streptomycin resistance marker. These strains were

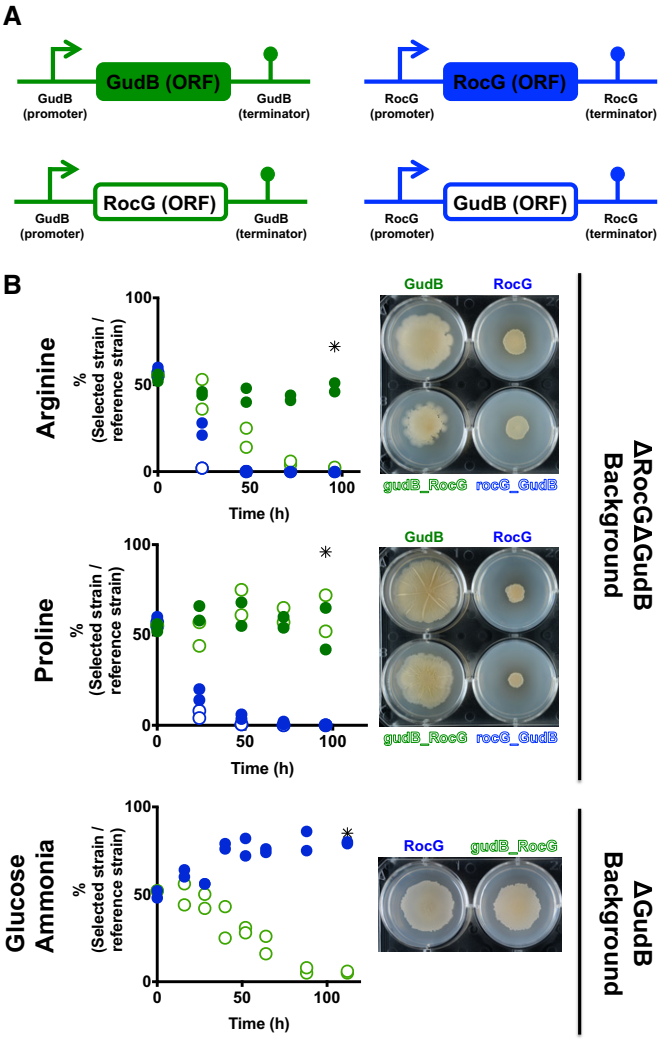

Figure 5. Swapping the regulatory and coding regions of *rocG* and *gudB* results in lower fitness.

A Schematic representation of the constructed swapped genes. Strains are marked by the standard colour code depending on their regulatory region (GudB in green, RocG in blue). Full green and blue boxes correspond to wild-type genes with the cognate promoters and ORFs (shown in B as full circles (growth curves) or ordinary font (agar plates)). The open green box represents RocG ORF under GudB promoter/terminator, and the open blue box represents GudB ORF under RocG promoter/terminator (shown in B as open circles and hollow fonts). The gene constructs shown were inserted at a neutral landing site, in a strain having none of the wild-type genes (Δ*rocG*_Δ*gudB*) or wild-type RocG (Δ*gudB*).

B Strains carrying the original genes and swapped constructs were individually competed against a wild-type-like reference strain. Shown is the % of the competing strain (streptomycin resistance) for each passage along the 5-day experiments. The asterisk (*) denotes the frequencies observed in a calibrating experiment, namely, competing the wild-type strain that was applied as the reference in the competitions against an identical strain carrying a streptomycin resistance marker. The results of two independent biological replicates were plotted. Circle colours as in (A). Photographs of the colonies on solid agar were taken as specified in Materials and Methods.

individually competed against a reference strain—wild-type expressing an erythromycin resistance marker. Tested strains were individually mixed with the reference strain at equal proportions and then

grown by serial passages for 5 days. Their relative frequencies, in the initial mix and after growth, were determined by plating aliquots of the cultures on plates containing either streptomycin or erythromycin. As control, a wild-type strain expressing the streptomycin resistance marker was also competed against the reference strain. The latter exhibits a slight growth disadvantage relative to the streptomycin marker in the competing strains (Appendix Fig S4). However, the tested lines were all competed against the same reference strain thus allowing the comparison of the original genes to the swapped ones (Fig 5A).

Competitions were done initially in the Δ*gudB*_Δ*rocG* background, so as to analyse separately the effects of swaps in RocG versus GudB. Note that the intact GudB gene (full green circles) has lower fitness than the reference strain (asterisk). This is because the former comes at Δ*gudB*_Δ*rocG* background, and is therefore equivalent to Δ*rocG*. Accordingly, the wild-type RocG construct (full blue) being equivalent to Δ*gudB* has even lower fitness. These observations in effect duplicate the results of Fig 3. However, what the swapped genes indicate is that the exchange of ORFs results in an even higher fitness loss (Fig 5B, compare full to open circles of the same colour).

For example, in arginine (Fig 5B, top panel), by the end of the serial passage (100 h), the swapped gene where GudB's ORF was replaced with that of RocG (open green) was completely lost, while the frequency of the wild-type gene (GudB's ORF; full green) remained unchanged. If the key to regulation were transcription alone, then replacement of the enzymes (ORFs) would not have resulted in such a fitness loss, let alone if GudB's enzymatic rate is even higher than RocG's (Fig 4). The same is observed when RocG's ORF is replaced by GudB's (compare full to open blue, Fig 5B, to panel, 25 h).

The differences in ORFs are insufficient to account for the regulation of these two paralogues. For example, placing GudB's ORF under RocG's regulatory regions also causes a dramatic fitness loss (open blue, compared to full green circles; in both arginine and proline). Overall, in arginine, and to a lesser extent in proline, both the constitutive expression of RocG (i.e. under GudB's promoter/terminator) and the regulated expression of GudB (under RocG's promoter/terminator) resulted in low fitness. The level of promoter–enzyme incompatibility was, however, medium dependent. In proline, transcriptional regulation seems to play a more important functional role, since replacing the ORFs had a smaller effect than the one described in arginine (Fig 5B, mid panel).

The effect of swapped genes was also tested when both genes are present (i.e. using single knockout backgrounds). In media containing arginine or proline, the effect of swapping was less pronounced compared to the double knockout background, but the same trends were observed; meaning lower fitness was observed in strains carrying swapped genes relative to wild-type counterparts (Appendix Fig S3). However, in glucose–ammonia medium, replacing GudB's ORF with RocG results in a dramatic loss of fitness (Fig 5B, bottom panel). This is despite the fact that neither RocG nor GudB contribute to fitness in glucose–ammonia, as judged by the knockouts (Fig 3, top panel). Further, what this experiment also shows is that a strain with two wild-type RocG genes (full blue) behaves like wild-type (asterisk). Thus, under its original promoter, RocG is not deleterious even when duplicated. However, the expression of RocG under GudB's regulatory regions (open green) is highly deleterious.

Overall, the expression of the RocG enzyme under GudB's promoter (open green circles) is deleterious, in both arginine and glucose–ammonia media. Having GudB expressed under RocG's promoter is also deleterious, with both proline and arginine as nitrogen and carbon sources. The swap experiments therefore indicate that the regulatory and the coding regions of RocG and GudB coevolved.

GudB and RocG show different oligomeric stability and regulation

The promoter–enzyme swap experiments indicated that RocG and GudB must differ at the protein level. However, the differences observed in k_{cat}/K_M (Fig 4) did not account for this incompatibility. For example, expression of RocG under GudB's promoter resulted in excessive GDH activity (growth inhibition on glucose–ammonia, when GDH activity is redundant). This result suggests that, as opposed to the k_{cat}/K_M values, RocG is more active than GudB, at least under some conditions. Catabolic GDHs of eukaryotic organisms have been better characterized than their bacterial counterparts and were found to have complex allosteric regulation [18]. Most of the reported eukaryotic allosteric effectors we tested had no effect, except for ATP (and ADP, though to a lesser extent) and 2-oxoglutarate (the product of the reaction), which equally inhibited both enzymes. In all cases, the effects of allosteric regulation were relatively minor (Appendix Fig S5A).

While performing kinetics, we observed that the rates of product release decayed faster than expected, in particular for GudB. Addition of 10% glycerol to the enzyme stocks and reaction mixtures alleviated this decay (detailed analysis is provided below). Additionally, the reaction rates varied depending on the enzyme concentration in the stock solution prior to its addition to the reaction mixture, and it was not until glutamate was added to the stock solution that we observed maximal initial rates (as in the determination of k_{cat} and K_M values; Fig 4). These observations are consistent with GDHs being active only as hexamers, and also that the stability of their hexameric assembly is marginal [28,29]. We thus examined the hexamer stability of both GudB and RocG.

To quantify the effect of glutamate as a stabilizer of the active hexameric state, we incubated the enzyme stocks (2 μM monomer; throughout the text, enzyme concentrations relate to monomer concentrations) with 10% glycerol and varying concentrations of glutamate (0–200 mM, in accordance with the intracellular variability of glutamate in *B. subtilis* [30]). Initial rates were measured by diluting these stock solutions to a reaction mixture containing 10 mM glutamate, 4 mM NAD^+ and 10% glycerol, at a final enzyme concentration of 0.05 μM. The maximal initial rate, observed when the stock solution contained 200 mM glutamate, corresponds to the entire sample being in the active, hexameric state (as in Fig 5). As shown in Fig 6A, both GudB and RocG reach 100% active hexamers when preincubated with ≥ 100 mM glutamate. However, GudB's assembly is more dependent to glutamate concentrations than RocG. For example, at 20 mM glutamate, only 10% of GudB is assembled and active while RocG shows almost 50% of active hexamers.

We also noticed that pH can dramatically affect assembly, particularly of GudB. The intracellular pH of *B. subtilis* varies widely, from 6 up to 8, depending on cellular state and growth medium [31]. To measure the pH effect, the above-described experimental

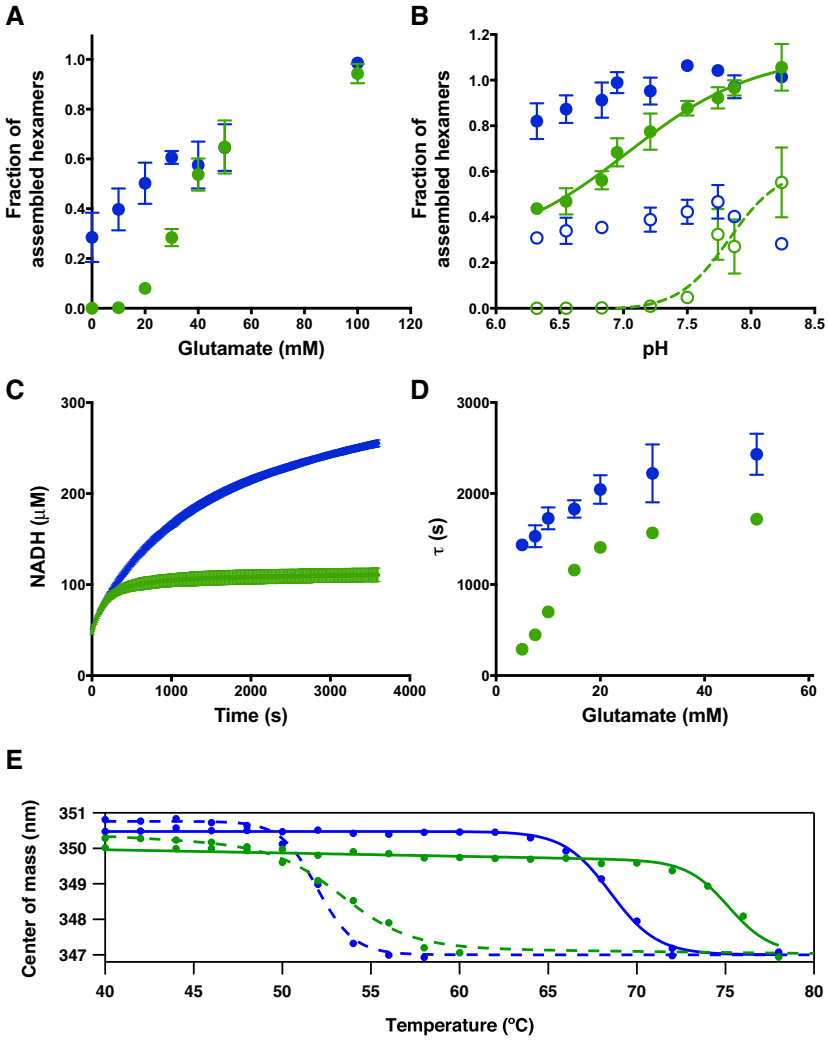

Figure 6. GudB activity is highly dependent on glutamate and pH.

A Hexameric assembly is glutamate dependent. Initial rates were measured from enzyme stocks incubated at the optimal pH (7.9) and varying concentrations of glutamate (0–200 mM). Enzymatic reactions were initiated by directly diluting to 0.05 μM final enzyme concentration in a reaction mixture containing 4 mM NAD^+ and 10 mM glutamate. The reactions' initial velocities were normalized to the maximal initial velocity (fully assembled enzyme, pre-incubated with 200 mM glutamate) and shown is the fraction of assembled hexamers versus glutamate concentration. Error bars represent the SD values from six experiments.

B GudB enzyme activity is pH dependent. Initial rates were measured from enzyme stocks incubated at two glutamate concentrations, 50 mM (open circles) and 200 mM (full circles) and varying pH (6.3–8.2). Enzymatic reactions and calculations were as described above (A). Error bars represent the SD values from three independent runs.

C Dissociation of hexamers in the course of the enzymatic reaction. Shown are enzymatic reactions initiated with pre-assembled enzymes (optimal pH and glutamate concentration), directly diluted to 0.05 μM final enzyme concentration in reaction mixes containing 4 mM NAD^+ and 5 mM glutamate. The line represents a fit to a single exponential decay ($V_t = (V_{t=0} + V_{t=\infty}) \times \exp(-kt) + V_{t=\infty}$). The derived decay time constants ($\tau = 1/k$) are 290 ± 25 s for GudB and 1,490 ± 30 s for RocG. Error bars represent the SD values from four independent runs.

D The dissociation decay time constants (τ) as a function of glutamate. The experiment as in panel (C) was repeated with varying concentrations of glutamate (5–50 mM). Presented is the time constant ($\tau = 1/k$) in relation to glutamate concentration in the reaction mixture. Error bars represent the SD values from four independent runs.

E Thermal unfolding curves, monitored by fluorescence, at 16 μM enzyme concentration in the absence (open circles and dotted lines) and presence of 250 mM glutamate (full circles and continues lines). As throughout the text, green and blue correspond to GudB and RocG, respectively. Lines show the fit of the data to the first equation in the section "Thermal denaturation assays" in Materials and Methods (see Materials and Methods from which the cooperativity constant (m) and apparent $T_{0.5}$ was calculated; full data set with varying enzyme concentrations and calculated m-values is shown in Appendix Fig S6B).

set-up was applied. Enzyme stocks were pre-incubated with 10% glycerol, 50 or 200 mM glutamate, and at varying pH (the glutamate dependency experiment, Fig 6A, had the stock solution at pH 7.9). As can be observed in Fig 6B, GudB's assembly is not only more dependent on glutamate, but also on pH, whereby protonation promotes dissociation. While RocG's assembly remained almost unaltered between pH 6 and 8, GudB fully dissociates if incubated at pH ≤ 7 and ≤ 50 mM glutamate. The apparent pK_a for dissociation

assembly is right within the physiological pH range, suggesting that pH is a regulator of GudB *in vivo*. The effects of pH and glutamate seem to be linked—high glutamate shifts to a lower pK_a, indicating that the deprotonated hexameric state is favoured by the glutamate-bound state (also, a significant fraction seems to be assembled in a pH-independent manner, at least in the range tested, a phenomena we cannot explain at present).

Irrespective of the enzymes' state in the stock solution, a more rapid than expected loss of activity was observed during the course of the enzymatic reaction itself, particularly at low glutamate concentrations. This loss was more pronounced in GudB compared to RocG (e.g. at 5 mM glutamate; Fig 6C). To quantify the relative dissociation propensity of GudB and RocG, the rates of product release were fitted to a first-order exponential decay. The decay rate constants indicated that the stability of GudB's oligomers is not only lower than that of RocG's (up to fivefold faster dissociation rates) but is also, as indicated in the previous experiments, more dependent on glutamate (Fig 6D). In this experimental setup, the largest differences between the two enzymes were observed at $\leq$ 50 mM glutamate and pH lower than 7.8. These rapid, exponential declines in the rates of product release are not due to product inhibition because the reaction products affect both enzymes weakly and to the same degree (Appendix Fig S5B). Nor can the observed decays be explained by the gradual depletion of NAD^+ and/or glutamate (see Materials and Methods).

Further support for regulation by hexameric assembly came from size-exclusion chromatography and thermal denaturation. Size-exclusion chromatography indicated that, at the range of enzyme concentration amenable for this analysis (1–16 μM), both RocG and GudB coexist in equilibrium of hexamers and lower order species (Appendix Fig S6A). In support of the kinetics presented above (obtained at a similar range 0.5–10 μM), the proportion of monomer–dimer–hexamer was dependent of on both protein and glutamate concentrations, with the active hexameric form being favoured at high protein and/or glutamate concentrations.

In agreement with the size-exclusion chromatography and kinetics, thermal denaturation experiments indicate that when highly concentrated, and in the presence of saturating glutamate concentrations, both enzymes show high unfolding temperatures ($T_{0.5} \geq 65$°C) and high cooperativity of unfolding (m-values $\geq$ 2.2 kJ/K/mol); Fig 6E and Appendix Fig S6B. At the lowest concentration that could be technically tested (0.8 μM), when both enzymes appeared largely monomeric by size-exclusion chromatography, the $T_{0.5}$ values were similarly low (~45°C). In this experiment, the only parameter that significantly differs between RocG and GudB is the magnitude of the stability shift upon glutamate binding to the hexameric state. The stability gain upon glutamate binding to the concentrated enzyme samples (16 μM) is significantly higher for GudB (ΔT of ~25°C versus 15°C for RocG). Further, the change in m-value, that reflects how cooperative unfolding is, upon glutamate binding is nearly twofold for GudB (from 1.4 to 2.6 kJ/K/mol) versus no change, or even lower cooperativity for RocG (from 2.6 with no glutamate to 2.2 kJ/K/mol) (Fig 6E and Appendix Fig S6B). Others reported that GDH's conformation and stability are dramatically dependent on glutamate [29]. The crystal structures of both GudB and RocG indicate hexamers can adopt two alternative monomer structures [32]. These observations are consistent with GudB's low unfolding cooperativity. However, the heterogeneity observed by size-exclusion chromatography at intermediate protein concentrations remains unclear. What is clear, however, is that glutamate binding is associated with a much larger change in the thermostability of GudB's hexameric state compared to RocG. This difference is consistent with the higher glutamate dependency of GudB's assembly, as seen in the kinetics experiments. The higher glutamate dependency of GudB is also manifested in more than six times higher K_M value compared to RocG, also in agreement with the processes of glutamate binding, hexameric assembly and enzymatic activity being coupled.

Altogether, our results indicate that GudB's constitutive transcription correlates with a tightly regulated enzyme, active only at relatively high glutamate concentrations. Further, even at saturating glutamate concentrations, maximal activity is only reached at pH 8, a value observed in *B. subtilis* cells during exponential phase [31]. Conversely, RocG's tight transcriptional regulation correlates with an enzyme that is less regulated, namely active at a wider range of glutamate concentration and pH. That GudB is a potentially more active enzyme than RocG (Fig 5) but whose activity is more tightly regulated, is fully consistent with the phenotypes of the promoter–enzyme swaps, and foremost with the inhibition of growth when GudB was placed under RocG's regulatory elements in a medium where GDH activity does not contribute to growth (Fig 5B).

Discussion

Incompatibility, or sign epistasis, is the hallmark of coevolution, indicating that evolutionary changes in separate loci are dependent on one another [33]. Epistasis dominates the divergence of both regulatory regions [34,35] and protein functions [36–39]. However, to our knowledge, promoter-ORF epistasis has been reported only once, in the evolution of antibiotics resistance [40], and its mechanistic basis remains unexplored. In RocG and GudB, all swaps resulted in dramatic loss of fitness, under at least one carbon–nitrogen source, but not across all sources. What is therefore likely to have led to this incompatibility, is a period of relaxed selection on one of these paralogues. Indeed, within species closely related to *B. subtilis*, RocG is frequently lost. RocG's function is limited to arginine utilization, while GudB's constitutive expression enables the utilization of multiple carbon and nitrogen sources including many metabolites that are catabolized via a glutamate intermediate. Thus, the "generalist" capacity of GudB to act at different environments might have enabled the loss of RocG [41]. Our findings suggest that GudB's "generalist" capability depends on a combination of constitutive expression and tight regulation of the enzymatic activity, by glutamate and intracellular pH, and possibly by other yet unknown factors.

That both RocG and GudB are tightly regulated, either transcriptionally or at the protein level, is in agreement with the finding that glutamate/glutamine/ammonia homoeostasis, and RocG in particular, is a key factor in *B. subtilis*, for maintenance of biofilm development [17] or under changes in osmotic pressure [42]. Glutamate homoeostasis also relates to glutamate synthase that is also tightly regulated [19]. RocG and GudB also regulate the levels of glutamate synthase [27] by binding to the transcription-activating factor GltC, thus blocking the expression of the glutamate synthase under conditions when *de novo* glutamate synthesis is not required [43]. Since GudB monomers are constantly present in the cell, even at low

glutamate concentrations (Fig 2), the interaction with GltC, and hence the regulation of expression of glutamate synthase, is also likely to relate to GudB's regulation of oligomeric assembly by glutamate and pH. This regulatory role of RocG and GudB may also augment the deleterious effect associated with RocG's expression under GudB's promoter when GDH activity is obsolete (Fig 5B, bottom panel).

GudB's mode of enzyme regulation—a transition from inactive dissociated monomers or/and dimers to enzymatically active hexamers, differs from the oft-described allosteric regulation. Although the majority of key metabolic enzymes are oligomers [44], the evidence for oligomeric assembly controlling enzyme function *in vivo* is so far limited to a few cases [45]. Direct imaging of dissociation and association of GudB in living bacteria would be most convincing. However, GudB and RocG cannot be tagged, *in vivo* neither at the C- or N-terminus (complete loss of activity due to inference with oligomer formation or disruption of the interaction with GltC [43]). Nonetheless, the *in vitro* data clearly indicate that GudB's association of enzymatically active hexamers is regulated by at least two physiologically relevant parameters—glutamate and pH. This transition may be simply driven by the glutamate-bound, deprotonated, hexameric form of GudB being thermodynamically favoured compared to the protonated, apo-form (as indicated by the thermal denaturation data, Fig 6E). Future studies may provide further insights regarding the structural details of this transition (the available crystal structures do indicate two different monomer configurations within the hexamers of both GudB and RocG; PDB codes: 3K8Z and 3K92) [32].

How common might be the co-evolutionary trend observed here? Transcriptomics enables systematic detection of functional divergence among regulatory regions [6]. However, functional changes in coding regions are not readily detected by high-throughput assays. This bias in detection capabilities also affect the assertion that changes in expression is the primary source of diversification [46]. In many cases, changes in regulation may well be the primary drive for divergence of a new paralogue [3], yet adaptive divergence in the coding region had followed [47]. Even more so, the scenario described here, namely coevolution of the regulatory and coding regions may be a frequent scenario rather than a rare exception. Such intrinsically correlated changes may be essential for maintaining paralogue-specific spatio-temporal control, especially in enzymes like GDHs that comprise metabolic hubs and in organisms with diverse ecology such as *B. subtilis*.

Materials and Methods

DNA manipulations

PCRs and plasmids were obtained by standard techniques using the Kapa HiFi ReadyMix polymerase (Kapa Biosystems), T4 DNA Ligase (Thermo) and restriction enzymes as needed (New England Biolabs). Primers are listed in Appendix Table S2, and the plasmids are described in Appendix Table S3. Genetically engineered *B. subtilis* strains (Appendix Table S4) were obtained by transformation based on natural competence. From a single colony of the parental strain, grown overnight at 37°C in LB agar plates, a 1 ml culture was started in the MC medium (0.5% glucose (Sigma), 1.4% K_2HPO_4 (Fisher Scientific), 0.6% KH_2PO_4 (Sigma), 30 nM sodium citrate tribasic dehydrate (Sigma), casein hydrolysate (Merck Millipore), ammonium iron (III) citrate (Sigma), L-glutamic acid potassium salt monohydrate (Sigma) and 3 μM $MgSO_4$ (Sigma)), modified from [48]. The culture was incubated for 4 h at 37°C in a roller drum shaker. After this time, 300 μl of the cell culture was mixed with 1 μg of DNA and incubated for 2 more hours under the same conditions. Selection for positive transformants was done in LB agar plates using the appropriate antibiotic. When linear DNA was used, flanking homology regions varied between 300 and 1,000 bp. Linear DNA was obtained from plasmids linearized with *Xho*I, or PCR products. Otherwise, genomic DNA of *B. subtilis* NCIB 3610 or PY79 strains that carried the desired genomic manipulation were used. All gene and genomic constructs were verified by DNA sequencing. To avoid the effect of hitchhiking mutations at other genomic loci, for each genomic construct, two individual, randomly chosen colonies were isolated, sequenced and assayed.

Media and growth conditions

Bacillus subtilis strains were grown in LB or minimal medium (MS) (5 mM potassium phosphate, 100 mM MOPS pH 7.1, 2 mM $MgCl_2$, 700 μM $CaCl_2$, 50 μM $MnCl_2$, 50 μM $FeCl_3$, 1 μM $ZnCl_2$, 2 μM thiamine, 50 μg/ml tryptophan, 50 μg/ml phenylalanine, 50 μg/ml threonine; adapted from [49]). The MS medium was supplemented with 0.5% ammonium sulphate and 0.5% glucose, or 0.5% proline, or 0.5% arginine. When required, media were supplemented with antibiotics: kanamycin (10 μg/ml), tetracycline (5 μg/ml), spectinomycin (100 μg/ml) or a mix of lincomycin (25 μg/ml) plus erythromycin (2 μg/ml). When required, the above liquid media were solidified through addition of Bacto agar (Difco) to 1.5%. To measure growth rates, 5 μl of starting culture (grown in LB medium with shaking at 37°C to mid-log phase) was used to inoculate 200 μl of the media tested. Growth was monitored in 96-well plates (Thermo Scientific) for 10–20 h at 30°C with shaking by measuring absorbance at 600 nm (Eon, BioTek). For growth on solid medium, 2 μl of starting culture (grown in LB medium with shaking at 37°C until mid-log phase) was spotted onto agar plates and incubated at 30°C for 3 days when proline, or glucose plus ammonia, was used as carbon and nitrogen sources, and 5 days with arginine. Photographs were taken using Nikon D800, F number 10.

Transcription levels

Reporter strains were grown 4–6 h in LB medium containing 100 μg/ml of streptomycin with shaking at 37°C, until $OD_{600\ nm}$ reached 0.8–1.0. 96-well plates were prepared with 200 μl of MS medium supplemented with 0.5% ammonium sulphate and 0.5% glucose, or 0.5% proline, or 0.5% arginine. The wells were inoculated with bacteria at a 1:200 dilution from the pre-culture. Cells were grown in the incubator with shaking (6 Hz) at 30°C for about 40 h. Every ~8 min, the plate was transferred by a robotic arm into a multi-well fluorimeter (Infinite F200, Tecan) that reads the $OD_{600\ nm}$ and $GFP_{480/535\ nm}$. Background fluorescence was subtracted from GFP measurements using as negative the non-fluorescent wild-type strain. Growth on solid medium was performed as previously described. Images were taken using a fluorescent stereoscope (Leica MZ16F). Images of wild-type strain not encoding the GFP reporter are shown in Appendix Fig S7. For FACS analysis, colonies of *B. subtilis* were resuspended in 5 ml phosphate saline buffer (PBS)

and sonicated at 30% power (VibraCell, Sonics) for 2 min at 10-s intervals. The cells were harvested by centrifugation and washed three times with PBS. The samples were analysed by flow cytometry (LSR-II, BD). A total of 10^6 cells were analysed. Based on the population with high fluorescence (GFP under GudB promoter/terminator in MS + proline), a gate of ~30,000 fluorescent cells was chosen and used for comparison. Statistics for gated cells and total events are shown in Appendix Table S5 and Appendix Fig S2.

Protein levels

Starting cultures of the analysed strains were obtained in LB medium with shaking at 37°C until $OD_{600\ nm}$ reached 0.8–1.0, after this a 1:200 dilution was performed into 100 ml of MS medium supplemented with 0.5% ammonium sulphate and 0.5% glucose, or 0.5% proline, or 0.5% arginine. Cultures were incubated at 30°C with shaking until $OD_{600\ nm}$ reached 0.8–1.0. Cells were harvested by centrifugation and resuspended in 1 ml of 100 mM Tris–HCl pH 7.6, 1 mM EDTA, 150 mM NaCl, 5% glycerol and protease inhibitor cocktail (Sigma; 500 times diluted). The cells were sonicated at 40% power (VibraCell, Sonics) for 4 min at 60-s intervals. The lysate was centrifuged at 38,720 *g* for 30 min. Protein concentration in the soluble fraction was measured using the Pierce BCA Protein Assay Kit (Thermo Scientific). The proteins were separated by 12% SDS–PAGE and transferred onto polyvinylidene difluoride membranes (Amersham Hybond-P, GE Healthcare). We used 5% milk in Tris-buffered saline plus 0.1% Tween 20 (TBS-T) for blocking and secondary antibody incubations, and 3% BSA in TBS-T was used for incubations with primary antibodies. A rabbit anti-RocG (1:10,000) [25] and anti-GudB (1:5,000) (kindly provided by Dr. Ulf Gerth) served as the primary antibody. The primary antibody was detected using anti-rabbit immunoglobulin G-peroxidase secondary antibodies (1:10,000) (Sigma) and the ECL System (GE Healthcare). Detection was performed using the ImageQuant LAS 4000 mini (GE Healthcare).

Growth competitions

Starting cultures of the competed strains were obtained in LB medium with shaking at 37°C until mid-log phase, after which a 1:1 mixture was prepared (by $OD_{600\ nm}$) and used to inoculate 10 ml of liquid MS medium. Cultures were grown at 30°C with shaking until $OD_{600\ nm}$ reached ~1.5–2. At this stage, a dilution of 1:100 was performed and growth was continued under the same conditions. Samples from these growth cultures were taken every 12 or 24 h, diluted in sterile LB media and plated on LB agar plates containing spectinomycin or mix of lincomycin (25 μg/ml) plus erythromycin (2 μg/ml). Colony-forming units were counted, and the ratio between spectinomycin- and erythromycin-resistant colonies was recorded. The results shown relate to the average of two parallel growth experiments (biological replicates) from each of which, two samples were taken for determination of strain ratio (technical replicates).

Enzyme expression and purification

E. coli BL21star/DE3 (pGRO7) was transformed with the expression plasmids pET28_Strep_GudB and pET28_Strep_RocG, encoding the wild-type *B. subtilis* enzymes with an N-terminus Strep-tag. *In vivo*, this tag had a deleterious growth effect, probably because it interrupts the interaction with GltC [43]. However, in our *in vitro* assays GltC binding is irrelevant. Cultures were grown in 500 ml of LB plus kanamycin (50 μg/ml) at 37°C to $OD_{600\ nm}$ = 0.6–0.8, induced with 0.5 mM IPTG and grown overnight at 20°C with shaking. Cells were harvested and resuspended in 40 ml of 100 mM Tris–HCl pH 7.6, 1 mM EDTA, 150 mM NaCl, 5% glycerol and protease inhibitor cocktail (Sigma; 500 times diluted). Following sonication (at 40% power, VibraCell, Sonics, for 4 min at 60-s intervals), the lysate was clarified by centrifugation (38,000 *g* for 30 min) and filtration. The enzymes were purified by affinity chromatography using gravity flow columns following the manufacturer's protocol (Iba Technologies). Glycerol (10%) was added to the elution and all subsequent solutions. Proteins were dialysed using the storage buffer (50 mM Hepes-KOH pH 7.9 and 10% glycerol) with 100 mM, or with no glutamate (monopotassium salt). In the absence of dialysis step, results of kinetic assays (Figs 5 and 6) were not reproducible, possibly due to the enzymes being purified with a native ligand that modulates oligomer stability. Proteins were analysed by SDS–PAGE (purity was ≥ 95% in all cases), concentrated to ~20 μM (all denoted protein concentrations relate to subunit concentrations) and stored at −80°C after fast freezing in liquid nitrogen.

Enzyme kinetics

Deamination of glutamate was assayed by measuring the increase in absorption at 340 nm (Eon, BioTek) due to the conversion of NAD^+ into NADH, in reaction buffer (50 mM Hepes pH 7.9 (KOH), 10% glycerol) and varying concentrations of glutamate (monopotassium salt, since sodium has an effect on GudB's activity), using 96-well plates suitable for UV range (Microplate UV/VIS 96F, Eppendorf). Throughout, we used 4 mM NAD^+. Total reaction volumes were 200 μl, and reactions were run at room temperature. To determine the kinetic parameters (k_{cat}, K_M), initial reaction rates were determined (e.g. Fig 5). To this end, 2 μM stock enzyme solutions (in a 50 mM Hepes pH 7.9 buffer with 10% glycerol and 100 mM glutamate) were directly diluted to the reaction buffer and varying glutamate concentrations. The final enzyme concentration was 0.05 μM. We repetitively observed a K_M value that is ~50-fold higher that reported in a previous enzymatic characterization of RocG [28] but matches the one reported later for the same enzyme [32]. The k_{cat} we measured for RocG was ~3.5-fold lower than reported [28]. These differences may relate to the concentration of NAD^+ in the reaction buffer. GDHs are known to exhibit complex rate dependencies with respect to NAD^+/NADH concentrations, and rates may not plateau at 1 mM [50]. Additionally, at concentrations below 5 mM glutamate, GudB lost all activity within the first 2 min of the reaction (Fig 6). The use of 10% glycerol in the reaction buffer was therefore crucial for reliably measuring initial rates, especially for GudB at low glutamate concentrations.

The loss of activity as the reaction progressed (Fig 6C and D) was ascribed to hexamer dissociation rather than to product inhibition or substrate consumption. The latter was excluded because at the substrate concentrations applied here, and the amount of substrate consumed in the course of reactions, the rate reduction expected by the Michaelis–Menten dependency on substrate concentrations ($v \propto [S]/(K_M+[S])$ is ≤ 6%; however, the observed rate decays are ≥ 90%. To assay the dissociation of hexamers (Fig 6D), a 2 μM enzyme stock solution in 50 mM Hepes, 10%

glycerol was incubated for 1–2 h at room temperature in varying concentrations of glutamate (5–200 mM) or at varying pH (6.5–8.2). Aliquots were added to 50 mM Hepes buffer pH 7.9, 10% glycerol, containing NAD^+ and glutamate (final concentrations 4 and 10 mM, respectively; enzyme at 0.05 μM). The reverse (glutamate synthase) reaction was similarly assayed by measuring the decrease in NADH absorption at 340 nm (Eon, BioTek) under varying concentrations of ammonium chloride, 1.5 mM NADH and 20 mM 2-oxoglutarate in 50 mM potassium phosphate pH 7.6 plus 10% glycerol.

Size-exclusion chromatography

Proteins were diluted to varying concentrations in equilibration buffer (100 mM Tris–HCl pH 7.6, 150 mM NaCl, 1 mM EDTA) with 200 mM glutamate (monosodium salt) or without. Samples volumes of 250 μl were loaded onto a Superdex 200 Increase 10/300 GL column (GE Healthcare) pre-equilibrated with the same buffer. The flow rate was 0.4 ml/min.

Thermal denaturation assays

Fluorescence emission spectrums were monitored using a Cary Eclipse Fluorescence spectrophotometer equipped with a Peltier-thermostatted holder. Excitation was at 280 nm, and emission was recorded between 300 and 400 nm. Samples were prepared by 20 times dilution from the appropriated stock solution in Tris buffer into 50 mM potassium phosphate at pH 7.6. Experiments were carried, for each protein concentration, at different temperatures within the range of 10–80°C (Appendix Fig S6B). The centre of spectral mass (CM) of individual spectra was defined as:

$$CM = \frac{\sum \lambda_i \cdot I_i}{\sum I_i},$$

where I_i is the fluorescence emitted at wavelength number λ_i. The change in the CM as a function of temperature was used to follow the denaturation process. Because RocG and GudB occupy intermediate states along the oligomerization pathway, a formal melting temperature could not be defined. As such, the inflection, midpoint point of the denaturation curve ($T_{0.5}$, in °K), and the cooperatively constant (m), were derived by fitting to a generic two state model that served for comparison of thermostabilities:

$$CM = \frac{x_N + x_D \cdot e^{\frac{m(T_{0.5}-T)}{R \cdot T}}}{\left(1 + e^{\frac{m(T_{0.5}-T)}{R \cdot T}}\right)},$$

where x_N relates to the spectral CM of the native state, that changes linearly with temperature ($x_N = \alpha_N + \beta_N \cdot T$), and x_D to the spectral CM of the denatured state ($x_D = \alpha_D + \beta_D \cdot T$).

Expanded View for this article is available online.

Acknowledgements

The authors thank Dr. Ulf Gerth and Prof. Jörg Stülke for kindly providing the anti-GudB and anti-RocG antibodies, respectively. We are grateful to Naama Barkai, Fabian Commichau, Moshe Goldsmith and Adriana Espinoza-Cantú for valuable comments regarding this manuscript. We thank Nitai Steinberg and Yaara Oppenheimer-Shaanan for their guidance regarding *B. subtilis* growth and genetic manipulations. Financial support by the Sasson and Marjorie Peress Fund is gratefully acknowledged. L.N.G. was supported by the CONACYT grant #203740 and the Martin Kurshner Fellowship, from Weizmann Institute of Science. M.L.R.R. was supported by the Ramon Areces Foundation. D.S.T. is the Nella and Leon Benoziyo Professor of Biochemistry.

Author contributions

LN-G and DST designed experiments, analysed data and wrote the manuscript. IK-G provided guidance and reagents regarding *B. subtilis* growth and genetic manipulations. LNG performed all experiments, except thermal denaturation performed by MLRR and optimization of the conditions for enzyme kinetics, performed by LML.

Conflict of interest

The authors declare that they have no conflict of interest.

References

1. Jacob F, Monod J (1961) Genetic regulatory mechanisms in the synthesis of proteins. *J Mol Biol* 3: 318 – 356
2. Pushker R, Mira A, Rodriguez-Valera F (2004) Comparative genomics of gene-family size in closely related bacteria. *Genome Biol* 5: R27
3. Hittinger CT, Carroll SB (2007) Gene duplication and the adaptive evolution of a classic genetic switch. *Nature* 449: 677 – 681
4. Gu ZL, Nicolae D, Lu HHS, Li WH (2002) Rapid divergence in expression between duplicate genes inferred from microarray data. *Trends Genet* 18: 609 – 613
5. Wang J, Marowsky NC, Fan CZ (2013) Divergent evolutionary and expression patterns between lineage specific new duplicate genes and their parental paralogs in *Arabidopsis thaliana*. *PLoS ONE* 8: e72362
6. Soria PS, McGary KL, Rokas A (2014) Functional divergence for every paralog. *Mol Biol Evol* 31: 984 – 992
7. Panchin AY, Gelfand MS, Ramensky VE, Artamonova II (2010) Asymmetric and non-uniform evolution of recently duplicated human genes. *Biol Direct* 5: 54
8. Pegueroles C, Laurie S, Alba MM (2013) Accelerated evolution after gene duplication: a time-dependent process affecting just one copy. *Mol Biol Evol* 30: 1830 – 1842
9. Kondrashov FA, Rogozin IB, Wolf YI, Koonin EV (2002) Selection in the evolution of gene duplications. *Genome Biol* 3: RESEARCH0008
10. Castillo-Davis CI, Hartl DL, Achaz G (2004) cis-Regulatory and protein evolution in orthologous and duplicate genes. *Genome Res* 14: 1530 – 1536
11. Wagner A (2000) Decoupled evolution of coding region and mRNA expression patterns after gene duplication: implications for the neutralist-selectionist debate. *Proc Natl Acad Sci USA* 97: 6579 – 6584
12. Penalosa-Ruiz G, Aranda C, Ongay-Larios L, Colon M, Quezada H, Gonzalez A (2012) Paralogous ALT1 and ALT2 retention and diversification have generated catalytically active and inactive aminotransferases in *Saccharomyces cerevisiae*. *PLoS ONE* 7: e45702
13. Quezada H, Aranda C, DeLuna A, Hernandez H, Calcagno ML, Marin-Hernandez A, Gonzalez A (2008) Specialization of the paralogue LYS21 determines lysine biosynthesis under respiratory metabolism in *Saccharomyces cerevisiae*. *Microbiol-Sgm* 154: 1656 – 1667
14. DeLuna A, Avendano A, Riego L, Gonzalez A (2001) NADP-glutamate dehydrogenase isoenzymes of *Saccharomyces cerevisiae* - Purification, kinetic properties, and physiological roles. *J Biol Chem* 276: 43775 – 43783
15. Lopez G, Quezada H, Duhne M, Gonzalez J, Lezama M, El-Hafidi M, Colon M, Martinez de la Escalera X, Flores-Villegas MC, Scazzocchio C

et al (2015) Diversification of paralogous alpha-isopropylmalate synthases by modulation of feedback control and hetero-oligomerization in *Saccharomyces cerevisiae*. *Eukaryot Cell* 14: 564 – 577

16. Belitsky BR, Sonenshein AL (1998) Role and regulation of *Bacillus subtilis* glutamate dehydrogenase genes. *J Bacteriol* 180: 6298 – 6305
17. Liu J, Prindle A, Humphries J, Gabalda-Sagarra M, Asally M, Lee DY, Ly S, Garcia-Ojalvo J, Suel GM (2015) Metabolic co-dependence gives rise to collective oscillations within biofilms. *Nature* 523: 550 – 554
18. Smith TJ, Stanley CA (2008) Untangling the glutamate dehydrogenase allosteric nightmare. *Trends Biochem Sci* 33: 557 – 564
19. Gunka K, Commichau FM (2012) Control of glutamate homeostasis in *Bacillus subtilis*: a complex interplay between ammonium assimilation, glutamate biosynthesis and degradation. *Mol Microbiol* 85: 213 – 224
20. Belitsky BR, Kim HJ, Sonenshein AL (2004) CcpA-dependent regulation of *Bacillus subtilis* glutamate dehydrogenase gene expression. *J Bacteriol* 186: 3392 – 3398
21. Chumsakul O, Takahashi H, Oshima T, Hishimoto T, Kanaya S, Ogasawara N, Ishikawa S (2011) Genome-wide binding profiles of the *Bacillus subtilis* transition state regulator AbrB and its homolog Abh reveals their interactive role in transcriptional regulation. *Nucleic Acids Res* 39: 414 – 428
22. Belitsky BR, Sonenshein AL (1999) An enhancer element located downstream of the major glutamate dehydrogenase gene of *Bacillus subtilis*. *Proc Natl Acad Sci USA* 96: 10290 – 10295
23. Ali NO, Jeusset J, Larquet E, Le Cam E, Belitsky B, Sonenshein AL, Msadek T, Debarbouille M (2003) Specificity of the interaction of RocR with the rocG-rocA intergenic region in *Bacillus subtilis*. *Microbiology* 149: 739 – 750
24. Choi SK, Saier MH Jr (2005) Regulation of sigL expression by the catabolite control protein CcpA involves a roadblock mechanism in *Bacillus subtilis*: potential connection between carbon and nitrogen metabolism. *J Bacteriol* 187: 6856 – 6861
25. Commichau FM, Wacker I, Schleider J, Blencke HM, Reif I, Tripal P, Stulke J (2007) Characterization of *Bacillus subtilis* mutants with carbon source-independent glutamate biosynthesis. *J Mol Microbiol Biotechnol* 12: 106 – 113
26. Zeigler DR, Pragai Z, Rodriguez S, Chevreux B, Muffler A, Albert T, Bai R, Wyss M, Perkins JB (2008) The origins of 168, W23, and other *Bacillus subtilis* legacy strains. *J Bacteriol* 190: 6983 – 6995
27. Stannek L, Thiele MJ, Ischebeck T, Gunka K, Hammer E, Volker U, Commichau FM (2015) Evidence for synergistic control of glutamate biosynthesis by glutamate dehydrogenases and glutamate in *Bacillus subtilis*. *Environ Microbiol* 17: 3379 – 3390
28. Khan MI, Ito K, Kim H, Ashida H, Ishikawa T, Shibata H, Sawa Y (2005) Molecular properties and enhancement of thermostability by random mutagenesis of glutamate dehydrogenase from *Bacillus subtilis*. *Biosci Biotechnol Biochem* 69: 1861 – 1870
29. Wacker SA, Bradley MJ, Marion J, Bell E (2010) Ligand-induced changes in the conformational stability and flexibility of glutamate dehydrogenase and their role in catalysis and regulation. *Protein Sci* 19: 1820 – 1829
30. Tempest DW, Meers JL, Brown CM (1970) Influence of environment on the content and composition of microbial free amino acid pools. *J Gen Microbiol* 64: 171 – 185
31. van Beilen JWA, Brul S (2013) Compartment-specific pH monitoring in *Bacillus subtilis* using fluorescent sensor proteins: a tool to analyze the antibacterial effect of weak organic acids. *Front Microbiol* 4: 157
32. Gunka K, Newman JA, Commichau FM, Herzberg C, Rodrigues C, Hewitt L, Lewis RJ, Stulke J (2010) Functional dissection of a trigger enzyme: mutations of the *Bacillus subtilis* glutamate dehydrogenase RocG that affect differentially its catalytic activity and regulatory properties. *J Mol Biol* 400: 815 – 827
33. de Visser JA, Krug J (2014) Empirical fitness landscapes and the predictability of evolution. *Nat Rev Genet* 15: 480 – 490
34. Emera D, Wagner GP (2012) Transformation of a transposon into a derived prolactin promoter with function during human pregnancy. *Proc Natl Acad Sci USA* 109: 11246 – 11251
35. Barriere A, Gordon KL, Ruvinsky I (2012) Coevolution within and between regulatory loci can preserve promoter function despite evolutionary rate acceleration. *PLoS Genet* 8: e1002961
36. Bridgham JT, Ortlund EA, Thornton JW (2009) An epistatic ratchet constrains the direction of glucocorticoid receptor evolution. *Nature* 461: 515 – 519
37. Lunzer M, Golding GB, Dean AM (2010) Pervasive cryptic epistasis in molecular evolution. *PLoS Genet* 6: e1001162
38. Wellner A, Gurevich MR, Tawfik DS (2013) Mechanisms of protein sequence divergence and incompatibility. *PLoS Genet* 9: e1003665
39. Boucher JI, Jacobowitz JR, Beckett BC, Classen S, Theobald DL (2014) An atomic-resolution view of neofunctionalization in the evolution of apicomplexan lactate dehydrogenases. *Elife* 3: e02304
40. Weinreich DM, Delaney NF, DePristo MA, Hartl DL (2006) Darwinian evolution can follow only very few mutational paths to fitter proteins. *Science* 312: 111 – 114
41. Noda-Garcia L, Camacho-Zarco AR, Medina-Ruiz S, Gaytan P, Carrillo-Tripp M, Fulop V, Barona-Gomez F (2013) Evolution of substrate specificity in a recipient's enzyme following horizontal gene transfer. *Mol Biol Evol* 30: 2024 – 2034
42. Kohlstedt M, Sappa PK, Meyer H, Maass S, Zaprasis A, Hoffmann T, Becker J, Steil L, Hecker M, van Dijl JM *et al* (2014) Adaptation of *Bacillus subtilis* carbon core metabolism to simultaneous nutrient limitation and osmotic challenge: a multi-omics perspective. *Environ Microbiol* 16: 1898 – 1917
43. Commichau FM, Herzberg C, Tripal P, Valerius O, Stulke J (2007) A regulatory protein-protein interaction governs glutamate biosynthesis in *Bacillus subtilis*: the glutamate dehydrogenase RocG moonlights in controlling the transcription factor GltC. *Mol Microbiol* 65: 642 – 654
44. Levy ED, Teichmann S (2013) Structural, evolutionary, and assembly principles of protein oligomerization. *Prog Mol Biol Transl Sci* 117: 25 – 51
45. Traut TW (1994) Dissociation of enzyme oligomers – a mechanism for allosteric regulation. *Crit Rev Biochem Mol* 29: 125 – 163
46. Voordeckers K, Pougach K, Verstrepen KJ (2015) How do regulatory networks evolve and expand throughout evolution? *Curr Opin Biotech* 34: 180 – 188
47. Lavy T, Yanagida H, Tawfik DS (2015) Gal3 binds Gal80 tighter than Gal1 indicating adaptive protein changes following duplication. *Mol Biol Evol* 33: 472 – 477
48. Wilson GA, Bott KF (1968) Nutritional factors influencing the development of competence in the *Bacillus subtilis* transformation system. *J Bacteriol* 95: 1439 – 1449
49. Branda SS, Gonzalez-Pastor JE, Ben-Yehuda S, Losick R, Kolter R (2001) Fruiting body formation by *Bacillus subtilis*. *Proc Natl Acad Sci USA* 98: 11621 – 11626
50. Engel PC (2011) A marriage full of surprises: forty-five years living with glutamate dehydrogenase. *Neurochem Int* 59: 489 – 494
51. Rice DW, Hornby DP, Engel PC (1985) Crystallization of an NAD+-dependent glutamate dehydrogenase from *Clostridium symbiosum*. *J Mol Biol* 181: 147 – 149

